HHS Public Access

Author manuscript

Curr Biol. Author manuscript; available in PMC 2017 September 12.

Published in final edited form as:

Curr Biol. 2016 September 12; 26(17): 2301–2312. doi:10.1016/j.cub.2016.07.054.

Stimulation of the Pontine Parabrachial Nucleus Promotes Wakefulness via Extra-thalamic Forebrain Circuit Nodes

Mei Hong Qiu[1,2,3,*], **Michael C. Chen**[3], **Patrick M. Fuller**[3], and **Jun Lu**[3,*]

[1]Department of Neurobiology, School of Basic Medical Science, Fudan University, Shanghai 200032, China

[2]Department of Pharmacology, School of Basic Medical Science, Fudan University, Shanghai 200032, China

[3]Department of Neurology, Beth Israel Deaconess Medical Center and Harvard Medical School, Boston, MA 02115, USA

SUMMARY

Human and animal studies have identified an especially critical role for the brainstem parabrachial (PB) complex in regulating electrocortical (electroencephalogram [EEG]) and behavioral arousal: lesions of the PB complex produce a monotonous high-voltage, slow-wave EEG and eliminate spontaneous behaviors. We report here that targeted chemogenetic activation of the PB complex produces sustained EEG and behavioral arousal in the rat. We further establish, using viral-mediated retrograde activation, that PB projections to the preoptic-basal forebrain and lateral hypothalamus, but not to the thalamus, mediate PB-driven wakefulness. We exploited this novel and noninvasive model of induced wakefulness to explore the EEG and metabolic consequences of extended wakefulness. Repeated (daily) chemogenetic activation of the PB was highly effective in extending wakefulness over 4 days, although subsequent PB activation produced progressively lesser wake amounts. Curiously, no EEG or behavioral sleep rebound was observed, even after 4 days of induced wakefulness. Following the last of the four daily induced wake bouts, we examined the brains and observed a chimeric pattern of c-Fos expression, with c-Fos expressed in subsets of both arousal- and sleep-promoting nuclei. From a metabolic standpoint, induced extended wakefulness significantly reduced body weight and leptin but was without significant effect on cholesterol, triglyceride, or insulin levels, suggesting that high sleep pressure or sleep debt per se does not, as previously implicated, result in a deleterious metabolic phenotype.

Graphical abstract

*Correspondence: mhqiu@shmu.edu.cn (M.H.Q.), jlu@bidmc.harvard.edu (J.L.).

SUPPLEMENTAL INFORMATION

Supplemental Information includes Supplemental Experimental Procedures and can be found with this article online at http://dx.doi.org/10.1016/j.cub.2016.07.054.

AUTHOR CONTRIBUTIONS

M.H.Q. conceived, designed, and performed the experiments; analyzed the data; prepared the figures; and wrote the manuscript. M.C.C. contributed reagents and materials and wrote the paper. P.M.F. contributed reagents, interpreted results, and wrote the manuscript. J.L. conceived and designed the experiments and wrote the manuscript.

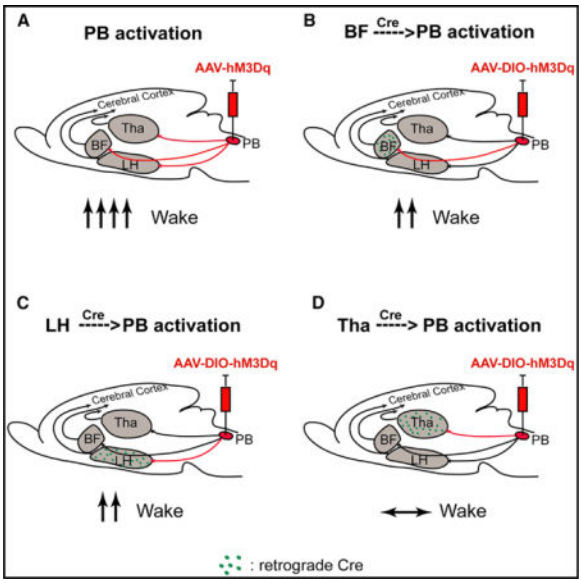

INTRODUCTION

The parabrachial complex (PB) of the dorsolateral pons provides extensive, largely glutamatergic, ascending innervation of the cerebral cortex, basal forebrain (BF), hypothalamus, thalamus, amygdala complex, and descending projections to medullary regions [1–4]. Together, these projections enable the PB to exert powerful control over a wide range of neurobiological functions, including thermoregulation, respiration, pain, fear, and feeding [5–7]. Inputs to the PB complex include most of its own targets as well as the spinal cord [2, 8, 9]. In its most fundamental neurobiological context, however, the PB plays an indispensable role in generating and maintaining electroencephalogram (EEG) arousal and behavioral wakefulness [10]. For example, cell-body-specific lesions of the medial PB (MPB) and lateral PB (LPB) in rats results in ~40% and ~10% reduction in wakefulness, respectively, whereas lesions encompassing the entire PB complex produce a coma-like state, i.e., a monotonous <1.0-Hz EEG and behavioral unresponsiveness. Genetically driven disruption of glutamate transmission by PB neurons also results in a large reduction in total wake and slowing of the waking EEG [11]. Thus, whereas lesions of the PB can dramatically reduce EEG and behavioral arousal, it remains unknown whether acute activation of the PB is sufficient to trigger and maintain EEG and behavioral arousal.

The circuit basis through which the PB might drive EEG and behavioral arousal also remains unclear. On the basis of our previous finding that lesions of both cholinergic and non-cholinergic corticopetal BF neurons result in coma [10], we proposed a PB-BF-cortex pathway as the structural basis by which the PB maintains EEG and behavioral arousal. It is the case, however, that the preoptic area (POA) hypothalamus, lateral hypothalamus (LH), and thalamus may also mediate PB control of wakefulness, as these forebrain structures are also densely innervated by the PB and, for the most part, provide direct innervation of the cortex [12]. To evaluate the role of these respective PB afferent pathways in arousal, we

employed, in combination, a viral-based retrograde and excitatory chemogenetic system to selectively activate the PB-POA-BF, PB-LH, and PB-thalamus pathways.

We finally asked whether chronic activation of the PB might provide a novel and noninvasive (i.e., absence of external stressor) way to extend wakefulness, as this would facilitate the assessment of the EEG and metabolic consequences of extended wakefulness per se. To this end, extended wakefulness in humans, by means of sleep restriction or deprivation, produced deleterious metabolic changes [13–16], whereas animal studies have provided mixed results [17, 18].

RESULTS

Chemogenetic Stimulation of the PB Induces a Long Wakefulness

To examine the effect of PB activation on EEG and behavioral wakefulness, we placed bilateral injections of an adeno-associated viral (AAV) vector containing an excitatory modified muscarinic G-protein-coupled receptor (AAV_{10}-Ef1α-hM3Dq-mCherry; hereafter, AAV-hM3Dq) into the PB of seven rats (Figure 1A) along with EEG/electromyogram (EMG) electrodes. Histological assessment revealed robust, bilateral hM3Dq (mCherry+) expression in PB neurons (Figures 1B and 1C) of the injected rats. In vivo activation of PB neurons expressing the hM3Dq receptors by the receptor agonist clozapine-N-oxide (CNO) (0.2 mg/kg) was verified by intense nuclear c-Fos immunostaining (black color or green fluorescent) within mCherry+ PB neurons (brown or red fluorescent; Figures 1b, 1b′, and 1c). The extent of hM3Dq+ somata in the PB from each case are outlined in Figures 1Di (single CNO intraperitoneal [i.p.] injection) and 1Dii (4 consecutive days i.p. injection). Figure 1E illustrates the timeline of procedures on animals.

Three weeks after surgery, we administered vehicle (i.p.; saline) at 9 a.m. and, 1 day later, CNO (i.p.; 0.2 mg/kg), also at 9 a.m., to the AAV-hM3Dq rats. The animals were housed under a 12:12 light-dark (LD), with L on at 7 a.m. As compared to saline injections, CNO injection at 9 a.m. in the rats produced ~11 hr of continuous wakefulness (Figures 2A and 2B, black, and Figure 2C, the red-colored hourly time course of wakefulness). As compared with spontaneous wakefulness (Figure 2A, a), the rats remained relatively behaviorally quiet but with increased EEG power in the 5.0-Hz theta band (Figures 2Bb and 2E, upper left) during CNO-induced wakefulness. We analyzed the fast Fourier transform (FFT) spectra of each behavioral state (wake, non-rapid eye movement [NREM], and rapid eye movement [REM]) during and following CNO-induced wakefulness (Figures 2B and 2C, the red-colored one) using two time windows: 9 a.m.–9 p.m. (0–12 hr post-injection) and 9 p.m.–7 a.m. (12–22 hr post-injection). During the first 12 hr (9 a.m.–9 p.m.) after CNO injection, the average FFT of NREM sleep was reduced in the 0- to 3-Hz (delta) and 7- to 8-Hz (theta; Figure 2E, middle left) frequency ranges; no significant change was seen in the FFT of REM sleep (Figure 2E, bottom left). During the subsequent 9 p.m.–7 a.m. period, the reduced low-frequency power of NREM sleep (0–5.5 Hz) was still present (Figure 2E, middle right), the FFT of wake did not completely return to the pattern resembling baseline (Figure 2E, top right), and the REM sleep FFT was virtually identical to the baseline level (Figure 2E, bottom right). Despite the prolonged wakefulness, no EEG or behavioral sleep rebound (i.e., increased low-frequency power in the FFT of NREM sleep or increased behavioral sleep;

Figures 2C–2E) was observed during the night following the arousal effects of CNO. These results indicate that activation of hM3Dq+ PB neurons by CNO has a long-lasting effect on behavior arousal and an even longer effect on the EEG, in particular during NREM sleep.

One week after the behavioral experiments, and so that we could examine the pattern of post-CNO neuronal activity, we again injected animals with CNO at 9 a.m. but this time perfused them 4 hr later (1 p.m.). Consistent with the CNO-induced EEG and behavioral arousal, c-Fos was highly expressed in the cerebral cortex (Figure 3A, i and ii), dorsal striatum (Figure 3A, i and iii), intralaminar thalamus (Figure 3B, i and ii), posterior LH (pLH) (Figure 3B, i and iii), parasubthalamic nucleus (PSTh) (Figure 3C, i), orexin neurons (Figure 3D, i and ii), BF cholinergic neurons (Figure 3E, i and iii), tuberomammillary nucleus (TMN) (Figure 3F, i), and locus coeruleus (LC) (Figure 3G, i). By contrast, very little to no c-Fos was observed within three identified sleep centers in the brain: the median preoptic nucleus (MnPO) (Figure 3H, i and iii); VLPO (Figures 3E, i and ii, and 3H, ii and iv); and parafacial zone (PZ) (a newly identified sleep promoting center; Figure 3I, i and ii). The overall c-Fos expression pattern after PB activation was consistent with strong activation of the brain's arousal circuitry and the observed extended behavioral wakefulness. The c-Fos results moreover indicate that activation of the PB had a generally inhibitory influence on putative sleep-promoting MnPO, VLPO, and PZ neurons.

Chemogenetic Stimulation of PB-BF-POA Pathway Promotes Wake Behavior

We next sought to define the circuit basis by which the PB might drive EEG and behavioral arousal. To this end, we have previously shown that, in the rat, the PB-BF-cortex route is critical for cortical arousal [10]. Here, we asked whether the PB might regulate the absolute time of waking via the BF exclusively or perhaps also via the hypothalamus and/or thalamus. Within the hypothalamus, both the POA and LH are involved in sleep-wake regulation and the PB innervates both regions. To first ascertain the relative contribution of the PB-POA pathway to the wake-promoting effects of PB activation, we placed bilateral injection of a retrograde viral vector (AAV_6-cre, which is taken up by the axonal terminals and retrogradely transported to the neuronal bodies) [19, 20] into the POA—including the MnPO and VLPO—as well as bilateral injections of cre-dependent AAV-hM3Dq into the PB of seven rats. In other words, this approach enabled us to selectively express the hM3Dq receptors in PB neurons that project to the BF and POA. Three weeks post-injection, EEG/EMG and video were recorded in all animals. Rats received saline injections at 9 a.m. and CNO injections at 9 a.m. the next day. A week later, rats were perfused at 11 a.m. after CNO injection at 9 a.m.

The AAV_6-cre injections were verified by cre immunostaining, which in the case of the POA injections invariably included some of the magnocellular BF, in addition to the entire POA (Figure 4A); expression of hM3Dq receptors in PB neurons was verified by directly visualizing the fusion reporter mCherry (red color) under the fluorescent microscope (Figures 4B–4E). During the period 9 a.m.–1 p.m., activation of the PB-preoptic pathway by CNO injection significantly increased wakefulness (Figures 5A and 5B) and decreased the EEG power density of NREM sleep in the frequency range of 1–2.5 Hz during the first 4 hr after CNO administration (Figure 5C, left panel). EEG power density of wakefulness and

REM sleep were not different from saline-injected control levels (Figure 5C, left panel). There was a trend of behavioral sleep rebound during 3 p.m.–6 p.m., but it did not reach statistical significance (Figure 5A). However, the NREM EEG power in the 2- to 4-Hz range was elevated during this period (Figure 5C, right panel), suggesting some EEG sleep rebound.

Chemogenetic Stimulation of the PB-LH Pathway Promotes Wake Behavior

We next sought to determine whether selective activation of the PB-LH pathway would also promote wakefulness. To do so, we injected AAV_6-cre into the pLH and AAV-hM3Dq into the PB of six rats. Cre immunostaining and the fluorescent reporter mCherry shown in Figures 4F–4J verified the AAV_6-cre injection sites in pLH (Figure 4F) and the hM3Dq expression in the PB (Figures 4G–4J). Activation of the PB-LH pathway by CNO significantly increased wakefulness (Figures 5D and 5E), reduced delta power, and increased power in the 6- to 7-Hz frequency range of NREM sleep during the 4-hr post-injection window, as compared with the EEG following saline injections (Figure 5F, left panel). The EEG power density of wakefulness and REM sleep were not altered (Figure 5F, left panel). Behavioral sleep rebound was observed during the night period but was not accompanied by EEG rebound (Figures 5D–5F, right panel).

Chemogenetic Activation of PB-Thalamic Pathway Does Not Affect Wake Behavior

Another major target of the PB is the midline and intralaminar thalamus, a subcortical structure long implicated in EEG and behavioral arousal [21–23]. To determine whether selective activation of the PB-thalamic pathway promotes wakefulness, we injected AAV_6-cre into the midline and intralaminar thalamus and cre-dependent AAV-hM3Dq into the PB of six rats. Figures 4K–4O show the AAV_6-cre injection sites in the thalamus and the hM3Dq expression within the PB. In sharp contrast to that seen following activation of the PB-BF-POA and PB-LH pathways, activation of the PB-thalamic pathway produced only a transient increase in wake (Figures 5G and 5H) and was without effect on EEG FFT during wake, NREM, or REM sleep (Figure 5I).

Effects of Extended Wakefulness on EEG and Behavioral Sleep-Wake and Underlying Sleep-Wake Circuitry

To examine the effects of extended wakefulness, i.e., presumptive high sleep pressure, on sleep-wake states, sleep rebound, and the EEG power spectra, we injected CNO at 9 a.m. for 4 consecutive days in seven rats and continuously recorded EEG/EMG. Four hours after the fourth CNO injection (9 a.m.), the rats were perfused (1 p.m.). With respect to the duration of wakefulness induced by CNO, we found that the induced wakefulness was progressively reduced from ~11 hr on the 1st day to 7 hr on the 2nd day and to 5 hr on the 3rd day (Figure 2C). It is of interest, however, that, in spite of the reduction in the magnitude of wake induction, no EEG or behavioral sleep rebound was observed on any of the days following dissipation of the CNO effect (Figures 2C and 2D, middle).

Similar to that observed following the initial injection of CNO, wake and NREM sleep FFT was altered following the second CNO injection, and again, the EEG effects persisted beyond that seen on waking behavior (Figure 6A). By the third CNO injection, the wake

FFT was gradually reduced but never returned to normal baseline wake FFT patterns (Figure 6A, upper panel). NREM sleep FFT remained altered by the third and fourth CNO injection (Figure 6A, middle panel), whereas the REM sleep FFT remained unaltered by repeated CNO injections (Figure 6A, lower panel).

To examine the persistence of CNO effects on the EEG, we analyzed the averaged FFT of each stage during the period from 7 to 9 a.m., which were the 2 hr prior to each CNO injection. Wake FFT during the 7–9 a.m. period, and so nearly a full day after the first and second CNO injections, continued to exhibit differences from the baseline FFT of the same period, whereas no differences between the wake FFT during the last 7–9 a.m. period and baseline (Figure 6B, upper panel) were observed, indicating that the waking EEG returned to baseline spectrum following the third CNO injection. On the other hand, the NREM sleep FFT continued to show lower delta power than the baseline level (Figure 6B, middle panel) 24 hr after the first, second, and third CNO injections. REM sleep FFT was not altered during any of the 7–9 a.m. post-CNO injection times. These results indicate that PB activation by CNO has a much-longer-lasting effect on the EEG activity than its effects on behavior and that sleep pressure progressively reduces the behavioral waking and FFT effects of CNO.

c-Fos expression in sleep-wake circuits after the fourth CNO injection was also markedly different from that observed following the first CNO injection. For example, c-Fos expression was high in neurons of the sleep-active VLPO (Figures 3E, iv and v, and 3H, vi and viii), MnPO (Figure 3H, v and vii), and PZ (Figure 3I, iii and iv) and low or absent in wake-active neurons of the striatum (Figure 3A, vi), LH (Figure 3B, vi), orexin neurons (Figure 3D, iii and iv), BF cholinergic neurons (Figure 3E, iv and vi), TMN (Figure 3F, ii), and LC (Figure 3G, ii). We counted the number of c-Fos immunoreactive neurons in identified sleep-wake active nuclei, i.e., VLPO, PZ, TMN, and LC, as well as determined the percentage of c-Fos+ neurons in both BF ChAT+ and LH orexin A+ neurons. As shown in Figures 3J and 3K, c-Fos expression was significantly higher in sleep-active neurons and significantly lower in wake-active neurons following the fourth CNO treatment. The foregoing pattern of c-Fos expression in fact resembles that of the sleep state. On the other hand, c-Fos expression in the cortex (Figure 3A, iv and v), thalamus (Figure 3B, iv and v), PSTh (Figure 3C, ii), and PB (Figure 6C) was much higher than that observed in the typical sleep condition, resembling instead that of a normal spontaneous wake c-Fos pattern.

Effects of Extended Wakefulness on Body Weight and Energy Metabolism

We finally examined the effects of extended wakefulness, and hence sleep loss, over 4 consecutive days on body weight and metabolic biomarkers. As compared with controls, the CNO-injected rats experienced a cumulative sleep loss of about 27 hr across the 4 days. Compared with controls, we found a significant reduction in body weight (baseline: 338.8 ± 6.5 g; CNO × 4: 318.5 ± 5.1 g; $p = 0.039$) and leptin (control: 2.4 ± 0.4 ng/ml; CNO × 4: 1.1 ± 0.2 ng/ml; $p = 0.013$) following the extended CNO-induced wakefulness. On the other hand, blood glucose (control: 148.7 ± 19.3 mg/dl; CNO × 4: 204.5 ± 9.1 mg/dl; $p = 0.035$) was increased (Figures 7A and 7B), whereas insulin levels were unchanged (Figure 7B), and

cholesterol and triglyceride levels showed a non-significant trend toward a reduction in the CNO-injected group (Figure 7C).

DISCUSSION

Our results show that acute, reversible chemogenetic stimulation of the rat PB results in the activation of arousal-related circuits and suppression of sleep-related circuits to produce a long-lasting continuous bout of behavioral wakefulness with a 5.0-Hz theta-rich EEG. The observed behavioral wakefulness took the form of alert but minimally active arousal, consistent with the observed 5.0-Hz theta-rich EEG, also termed “hippocampal type 2 theta” [24]. Surprisingly, given prevailing models of sleep homeostasis, neither an EEG nor behavioral sleep rebound was observed following the induced extended wakefulness. In fact, the NREM sleep period subsequent to CNO-induced wakefulness, which occurred at its usual time, showed a *reduction*, not increase, in EEG delta and theta power. The REM sleep EEG, on the other hand, was unaffected. With respect to the circuit basis by which the PB can trigger and maintain EEG and behavioral arousal, we found that selective chemogenetic activation of PB-BF-POA or PB-LH pathways induces 4 or 5 hr wakefulness, with normal wake FFT, and a subsequent sleep rebound. In sharp contrast, chemogenetic activation of the PB-thalamic pathway produced only a negligible increase in waking. Repeated daily activation of the PB for 4 days similarly induced long bouts of waking behavior, although the length of the induced wake bouts became progressively shorter from days 1 to 4 (day 1–4: 11, 7, 5, and 4 hr, respectively). The 5.0-Hz theta peak observed during the induced wake was also progressively reduced following each CNO injection, returning to its near-normal power during wake by the fourth CNO injection. The NREM sleep FFT effects after induced wakefulness, however, remained pronounced following all four daily CNO injections. Finally, despite high sleep pressure from repeated CNO-induced wake periods, no sleep rebound in sleep time or FFT change was ever observed. That these divergent effects on the sleep and wake EEG spectra are likely due to increasing sleep pressure, and not simply desensitization of the hM3Dq receptor, was strongly indicated by robust c-Fos expression in the sleep-promoting VLPO, MnPO, and PZ following the 4^{th} day of CNO injections. Finally, extended wakefulness taking the form of an extra ~27 hr of wakefulness over 4 days resulted in significant reductions in body weight and leptin, an increase in glucose, no change in insulin, and minor, non-significant changes in cholesterol and triglycerides. Collectively, these metabolic changes are inconsistent with chronic sleep loss per se, underlying deleterious metabolic changes, at least in the rodent.

In animals and humans alike, EEG and behavioral arousal depend critically upon the structural and functional integrity of the PB complex [10, 25]. With respect to the targets of the PB, i.e., the circuit basis by which the PB can trigger and maintain wake, our previous lesion study and the present study indicate that the cellular BF, a major target of the PB, exerts potent control over EEG arousal and, in a cell-type-specific manner, behavioral arousal [10, 26]. On the other hand, multiple lesion studies have shown that the thalamus, also a major target of the PB, is not critical for normal levels of wakefulness nor is selective activation of glutamatergic thalamocortical neurons sufficient to drive wakefulness [10, 26, 27]; the results of the present study confirm and extend these prior findings concerning thalamic control of arousal. Our results, in combination with more-recent findings on the

cellular BF [26, 28], suggest that the reduced power in the lower-frequency EEG of NREM sleep and the pronounced 5-Hz theta rhythm during wakefulness following PB activation are likely driven by the PB-BF pathway, whereas behavioral wake is driven by activation of both the PB-BF-POA and PB-LH pathways, with little to no contribution from the PB-thalamus pathway. It is also of interest that the effects of PB activation on the NREM EEG persisted beyond the behavioral wake. This would suggest that EEG and behavioral wake were not completely synchronized and may link to differential activation of the ascending PB pathways. Dissociation of EEG and behavioral state has been previously described, most recently in studies showing that selective chemogenetic activation of BF cholinergic neurons produces a wake-like EEG during NREM sleep, but not behavioral wake [26, 28].

Whereas our retrograde circuit activation studies continue to support a key role for the BF in mediating much of the PB's EEG and behavioral arousal effect, our retrograde activation and c-Fos findings suggest that the POA and LH are also important circuit elements in these processes. With respect to the POA, both the VLPO and MnPO contain sleep-active neurons [29, 30] that are inhibitory (GABA and/or galanin) and project mainly to wake-promoting neurons of the LH and posterior hypothalamus (PH) [31, 32]. The cellular LH, on the other hand, is quite heterogeneous, containing orexin, melanin-concentrating hormone (MCH), GABAergic, nitric oxide (NO), and glutamate neurons, all of which have also been implicated in wake, NREM, and/or REM sleep [33–40]. The cellular PH is likewise heterogeneous, with the TMN neurons being its most notably resident population linked with arousal control. Non-selective cell body lesions of the LH that include the PH increase total sleep time by about 25% [12]. This marked increase in sleep time following LH+PH lesions is much higher than that seen following selective lesions or disruption of known LH and PH cell populations, e.g., orexin, MCH, histamine, etc. [41, 42]. Hence, another as yet unidentified population of arousal neurons in the LH and/or PH is likely operative, and findings from the present study would suggest that these putative unidentified arousal-promoting LH/PH neurons likely receive PB inputs and may work jointly with POA neurons to regulate arousal. To this end, activation of the PB-BF-POA pathway appears to inhibit both the MnPO and VLPO, which is interesting given that the inputs from the PB are presumptively glutamatergic and thus excitatory. It may therefore be the case that inhibition of the MnPO and VLPO is mediated by PB excitation of GABAergic interneurons or direct modulation of GABAergic terminals on VLPO and MnPO sleep neurons. Indeed, the ability of the PB to robustly produce sustained wake may ultimately require simultaneous stimulation of wake-active neurons in the BF and LH/PH *as well as* inhibition of POA sleep neurons, ultimately reflecting multiple circuit "layers" of arousal control. Finally, the extent to which "selective" retrograde activation of the PB-LH/PH pathway may have also activated the PB-POA-BF pathway, or vice versa, remains an open question. In other words, it is possible that the retrograde-based activation of PB neurons from the LH/PH or VLPO/POA may have also resulted in the activation of the other circuit via collaterals of the PB projection neurons. We attempted to examine this possibility through mapping of c-Fos but were unable to make a definite determination one way or the other. Given, however, the results of the PB-thalamus retrograde activation, which did not produce waking, we would argue that collaterals from the primary PB projections neurons are unlikely to contribute meaningfully to the responses observed.

The extended wakefulness induced by serial PB activations produced a significant sleep debt and, hence, presumably, high sleep pressure but had opposing effects on sleep- (VLPO and PZ) and wake-regulatory neurons (TMN, LC, orexin, and BF cholinergic neurons). And this high sleep pressure—secondary to extended wakefulness—progressively reduced waking time and power in the 5.0-Hz theta band induced by CNO, i.e., PB activation. Moreover, persisting effects on the wake and NREM sleep EEG FFT were observed beyond that of behavioral waking. Hence, the effect of increasing sleep pressure on the duration of arousal is consistent with an underlying sleep homeostat, but the absence of a sleep rebound in total sleep time or increased slow-wave EEG power following PB stimulation was highly surprising. In other words, the c-Fos observed in sleep-active neurons on day 4 is consistent with high sleep pressure in the animals at this time, yet we failed to observe any EEG or behavioral sleep rebound. One possible explanation for this curious finding is that the EEG effects of PB activation persisted beyond the observed behavioral wake. Another possibility is that whereas the direct activation effect on the PB is confined to the typical 6- to 8-hr period of CNO-induced chemogenetic stimulation, the effects on target arousal circuitry may last longer than the CNO period and suppress sleep rebound.

Our results further suggest that sleep induction requires not only the activation of sleep systems but also the inactivation of key arousal circuits, whereas behavioral wakefulness only requires the activation of arousal systems. This, in turn, would suggest that the activity of the brain's arousal circuitry is the primary determinant of the level of EEG and behavioral arousal, whereas the sleep process is somewhat more permissive in nature, at least when the activity of sleep-active neurons isn't potentiated using chemogenetics or hypnotics [43–45]. From an anatomic standpoint, this has a certain intuitive appeal given that arousal systems are strongly interconnected and project widely across the neuraxis, whereas sleep systems, by and large, project more locally to nearby arousal circuits. These features suggest that these disparate populations of sleep-active neurons may not be capable of coordinating a global sleep state without arousal systems also being inactive secondary to sleep pressure, circadian regulation, or lack of inputs. From a clinical standpoint, this model of sleep-wake regulation would square well with the hypothesis that primary insomnia might reflect a state of brain hyper-arousal rather than dysfunction of sleep-promoting circuitry. Hence, drugs targeting the brain's arousal circuitry, rather than potentiating sleep circuitry, may prove more efficacious in treating primary insomnia, as has been previously hypothesized [46].

The CNO-induced extended wakefulness in our rat model offers an experimental analog of human chronic sleep restriction, which is experienced at epidemic levels in modern society. Following 4 days of chronic sleep loss, we observed a significant reduction in body weight and leptin, an increase in blood glucose, no change in insulin, and non-significant reductions in blood cholesterol and triglyceride. These metabolic findings are generally consistent with those previously reported in rats who demonstrated chronic sleep loss but only minor, non-deleterious metabolic changes, secondary to lesions of the VLPO [18]. These prior findings, as well as those of the present study, are therefore a challenge to reconcile with human findings showing that sleep deprivation results in obesity and adverse metabolic changes [14–16]. One possible explanation for these disparate results between rodents and humans may link to the different waking metabolic rates of humans and rodents. On the other hand, there are likely factors associated with sleep deprivation or restriction in humans, including

stress and hedonic drives, which may contribute to the deleterious metabolic changes seen in humans following extended wakefulness. A human model of wake extension employing repeated administration of a wake-promoting compound, such as armodafinil, could potentially minimize the stress confound inherent to the human studies and provide a better direct comparison of wake-extension/sleep-loss (as the isolated variable) between the animal and human work.

In conclusion, we show for the first time that the pontine PB can potently drive cortical arousal and wake behavior and that either the PB-POA-BF or PB-LH/PH ascending circuit pathways are sufficient to mediate, to a large degree, these responses. By contrast, the PB-thalamic pathway does not appear to contribute meaningfully to the EEG and behavioral responses produced by PB activation. We further show that repeated (daily) injections of CNO represent a novel and noninvasive model of extended wakefulness that may have great utility in elucidating the neurocognitive, physiologic, and metabolic consequences of sleep loss per se.

Supplementary Material

Refer to Web version on PubMed Central for supplementary material.

Acknowledgments

This work was supported by the NIH (NS062727, NS061849, and NS 095986, to J.L.; NS073613 and NS092652, to P.M.F.), the National Natural Science Foundation of China (31171049, to M.H.Q.), and by the Scientific Research Foundation for Returned Overseas Chinese Scholars, State Education Ministry (to M.H.Q.).

References

1. Fulwiler CE, Saper CB. Subnuclear organization of the efferent connections of the parabrachial nucleus in the rat. Brain Res. 1984; 319:229–259. [PubMed: 6478256]
2. Herbert H, Moga MM, Saper CB. Connections of the parabrachial nucleus with the nucleus of the solitary tract and the medullary reticular formation in the rat. J Comp Neurol. 1990; 293:540–580. [PubMed: 1691748]
3. Saper CB. Reciprocal parabrachial-cortical connections in the rat. Brain Res. 1982; 242:33–40. [PubMed: 7104731]
4. Saper CB, Loewy AD. Efferent connections of the parabrachial nucleus in the rat. Brain Res. 1980; 197:291–317. [PubMed: 7407557]
5. Chamberlin NL. Functional organization of the parabrachial complex and intertrigeminal region in the control of breathing. Respir Physiol Neurobiol. 2004; 143:115–125. [PubMed: 15519549]
6. Morrison SF. 2010 Carl Ludwig Distinguished Lectureship of the APS Neural Control and Autonomic Regulation Section: Central neural pathways for thermoregulatory cold defense. J Appl Physiol. 2011; 110:1137–1149. [PubMed: 21270352]
7. Neugebauer V. Amygdala pain mechanisms. Handbook Exp Pharmacol. 2015; 227:261–284.
8. Fonseca AC, Geraldes R, Pires J, Falcão F, Bentes C, Melo TP. Improvement of sleep architecture in the follow up of a patient with bilateral paramedian thalamic stroke. Clin Neurol Neurosurg. 2011; 113:911–913. [PubMed: 21676536]
9. Moga MM, Herbert H, Hurley KM, Yasui Y, Gray TS, Saper CB. Organization of cortical, basal forebrain, and hypothalamic afferents to the parabrachial nucleus in the rat. J Comp Neurol. 1990; 295:624–661. [PubMed: 1694187]
10. Fuller PM, Sherman D, Pedersen NP, Saper CB, Lu J. Reassessment of the structural basis of the ascending arousal system. J Comp Neurol. 2011; 519:933–956. [PubMed: 21280045]

11. Kaur S, Pedersen NP, Yokota S, Hur EE, Fuller PM, Lazarus M, Chamberlin NL, Saper CB. Glutamatergic signaling from the parabrachial nucleus plays a critical role in hypercapnic arousal. J Neurosci. 2013; 33:7627–7640. [PubMed: 23637157]
12. Gerashchenko D, Kohls MD, Greco M, Waleh NS, Salin-Pascual R, Kilduff TS, Lappi DA, Shiromani PJ. Hypocretin-2-saporin lesions of the lateral hypothalamus produce narcoleptic-like sleep behavior in the rat. J Neurosci. 2001; 21:7273–7283. [PubMed: 11549737]
13. Banks S, Dinges DF. Behavioral and physiological consequences of sleep restriction. J Clin Sleep Med. 2007; 3:519–528. [PubMed: 17803017]
14. Huang PL. A comprehensive definition for metabolic syndrome. Dis Model Mech. 2009; 2:231–237. [PubMed: 19407331]
15. Knutson KL, Van Cauter E. Associations between sleep loss and increased risk of obesity and diabetes. Ann N Y Acad Sci. 2008; 1129:287–304. [PubMed: 18591489]
16. Spiegel K, Knutson K, Leproult R, Tasali E, Van Cauter E. Sleep loss: a novel risk factor for insulin resistance and type 2 diabetes. J Appl Physiol. 2005; 99:2008–2019. [PubMed: 16227462]
17. de Oliveira EM, Visniauskas B, Sandri S, Migliorini S, Andersen ML, Tufik S, Fock RA, Chagas JR, Campa A. Late effects of sleep restriction: Potentiating weight gain and insulin resistance arising from a high-fat diet in mice. Obesity (Silver Spring). 2015; 23:391–398. [PubMed: 25557274]
18. Vetrivelan R, Fuller PM, Yokota S, Lu J, Saper CB. Metabolic effects of chronic sleep restriction in rats. Sleep. 2012; 35:1511–1520. [PubMed: 23115400]
19. Towne C, Raoul C, Schneider BL, Aebischer P. Systemic AAV6 delivery mediating RNA interference against SOD1: neuromuscular transduction does not alter disease progression in fALS mice. Mol Ther. 2008; 16:1018–1025. [PubMed: 18414477]
20. Towne C, Schneider BL, Kieran D, Redmond DE Jr, Aebischer P. Efficient transduction of non-human primate motor neurons after intramuscular delivery of recombinant AAV serotype 6. Gene Ther. 2010; 17:141–146. [PubMed: 19727139]
21. Kinomura S, Larsson J, Gulyás B, Roland PE. Activation by attention of the human reticular formation and thalamic intralaminar nuclei. Science. 1996; 271:512–515. [PubMed: 8560267]
22. Maquet P, Péters J, Aerts J, Delfiore G, Degueldre C, Luxen A, Franck G. Functional neuroanatomy of human rapid-eye-movement sleep and dreaming. Nature. 1996; 383:163–166. [PubMed: 8774879]
23. Van der Werf YD, Witter MP, Groenewegen HJ. The intralaminar and midline nuclei of the thalamus. Anatomical and functional evidence for participation in processes of arousal and awareness. Brain Res Brain Res Rev. 2002; 39:107–140. [PubMed: 12423763]
24. Sainsbury RS, Harris JL, Rowland GL. Sensitization and hippocampal type 2 theta in the rat. Physiol Behav. 1987; 41:489–493. [PubMed: 3432404]
25. Parvizi J, Damasio AR. Neuroanatomical correlates of brainstem coma. Brain. 2003; 126:1524–1536. [PubMed: 12805123]
26. Anaclet C, Pedersen NP, Ferrari LL, Venner A, Bass CE, Arrigoni E, Fuller PM. Basal forebrain control of wakefulness and cortical rhythms. Nat Commun. 2015; 6:8744. [PubMed: 26524973]
27. Villablanca J, Salinas-Zeballos ME. Sleep-wakefulness, EEG and behavioral studies of chronic cats without the thalamus: the ‘athalamic’ cat. Arch Ital Biol. 1972; 110:383–411. [PubMed: 4349191]
28. Chen L, Yin D, Wang TX, Guo W, Dong H, Xu Q, Luo YJ, Cherasse Y, Lazarus M, Qiu ZL, et al. Basal forebrain cholinergic neurons primarily contribute to inhibition of electroencephalogram delta activity, rather than inducing behavioral wakefulness in mice. Neuropsychopharmacology. 2016; 41:2133–2146. [PubMed: 26797244]
29. Suntsova N, Szymusiak R, Alam MN, Guzman-Marin R, McGinty D. Sleep-waking discharge patterns of median preoptic nucleus neurons in rats. J Physiol. 2002; 543:665–677. [PubMed: 12205198]
30. Takahashi K, Lin JS, Sakai K. Characterization and mapping of sleep-waking specific neurons in the basal forebrain and preoptic hypothalamus in mice. Neuroscience. 2009; 161:269–292. [PubMed: 19285545]

31. Sherin JE, Elmquist JK, Torrealba F, Saper CB. Innervation of histaminergic tuberomammillary neurons by GABAergic and galaninergic neurons in the ventrolateral preoptic nucleus of the rat. J Neurosci. 1998; 18:4705–4721. [PubMed: 9614245]
32. Szymusiak R, McGinty D. Hypothalamic regulation of sleep and arousal. Ann N Y Acad Sci. 2008; 1129:275–286. [PubMed: 18591488]
33. Adamantidis AR, Zhang F, Aravanis AM, Deisseroth K, de Lecea L. Neural substrates of awakening probed with optogenetic control of hypocretin neurons. Nature. 2007; 450:420–424. [PubMed: 17943086]
34. Hara J, Beuckmann CT, Nambu T, Willie JT, Chemelli RM, Sinton CM, Sugiyama F, Yagami K, Goto K, Yanagisawa M, Sakurai T. Genetic ablation of orexin neurons in mice results in narcolepsy, hypophagia, and obesity. Neuron. 2001; 30:345–354. [PubMed: 11394998]
35. Hassani OK, Lee MG, Jones BE. Melanin-concentrating hormone neurons discharge in a reciprocal manner to orexin neurons across the sleep-wake cycle. Proc Natl Acad Sci USA. 2009; 106:2418–2422. [PubMed: 19188611]
36. Jego S, Glasgow SD, Herrera CG, Ekstrand M, Reed SJ, Boyce R, Friedman J, Burdakov D, Adamantidis AR. Optogenetic identification of a rapid eye movement sleep modulatory circuit in the hypothalamus. Nat Neurosci. 2013; 16:1637–1643. [PubMed: 24056699]
37. Lagos P, Torterolo P, Jantos H, Monti JM. Immunoneutralization of melanin-concentrating hormone (MCH) in the dorsal raphe nucleus: effects on sleep and wakefulness. Brain Res. 2011; 1369:112–118. [PubMed: 21078307]
38. Sasaki K, Suzuki M, Mieda M, Tsujino N, Roth B, Sakurai T. Pharmacogenetic modulation of orexin neurons alters sleep/wakefulness states in mice. PLoS ONE. 2011; 6:e20360. [PubMed: 21647372]
39. Tsunematsu T, Kilduff TS, Boyden ES, Takahashi S, Tominaga M, Yamanaka A. Acute optogenetic silencing of orexin/hypocretin neurons induces slow-wave sleep in mice. J Neurosci. 2011; 31:10529–10539. [PubMed: 21775598]
40. Tsunematsu T, Ueno T, Tabuchi S, Inutsuka A, Tanaka KF, Hasuwa H, Kilduff TS, Terao A, Yamanaka A. Optogenetic manipulation of activity and temporally controlled cell-specific ablation reveal a role for MCH neurons in sleep/wake regulation. J Neurosci. 2014; 34:6896–6909. [PubMed: 24828644]
41. Gerashchenko D, Chou TC, Blanco-Centurion CA, Saper CB, Shiromani PJ. Effects of lesions of the histaminergic tuberomammillary nucleus on spontaneous sleep in rats. Sleep. 2004; 27:1275–1281. [PubMed: 15586780]
42. Mochizuki T, Crocker A, McCormack S, Yanagisawa M, Sakurai T, Scammell TE. Behavioral state instability in orexin knockout mice. J Neurosci. 2004; 24:6291–6300. [PubMed: 15254084]
43. Anaclet C, Ferrari L, Arrigoni E, Bass CE, Saper CB, Lu J, Fuller PM. The GABAergic parafacial zone is a medullary slow wave sleep-promoting center. Nat Neurosci. 2014; 17:1217–1224. [PubMed: 25129078]
44. Becker PM, Somiah M. Non-benzodiazepine receptor agonists for insomnia. Sleep Med Clin. 2015; 10:57–76. [PubMed: 26055674]
45. Zisapel N. Drugs for insomnia. Expert Opin Emerg Drugs. 2012; 17:299–317. [PubMed: 22681198]
46. Cano G, Mochizuki T, Saper CB. Neural circuitry of stress-induced insomnia in rats. J Neurosci. 2008; 28:10167–10184. [PubMed: 18829974]

Highlights

- Chemogenetic activation of the PB induces continual wakefulness without sleep rebound
- The basal forebrain and hypothalamus, not thalamus, mediate PB-driven arousal
- Chronic PB-driven arousal produces only minor, non-deleterious metabolic changes

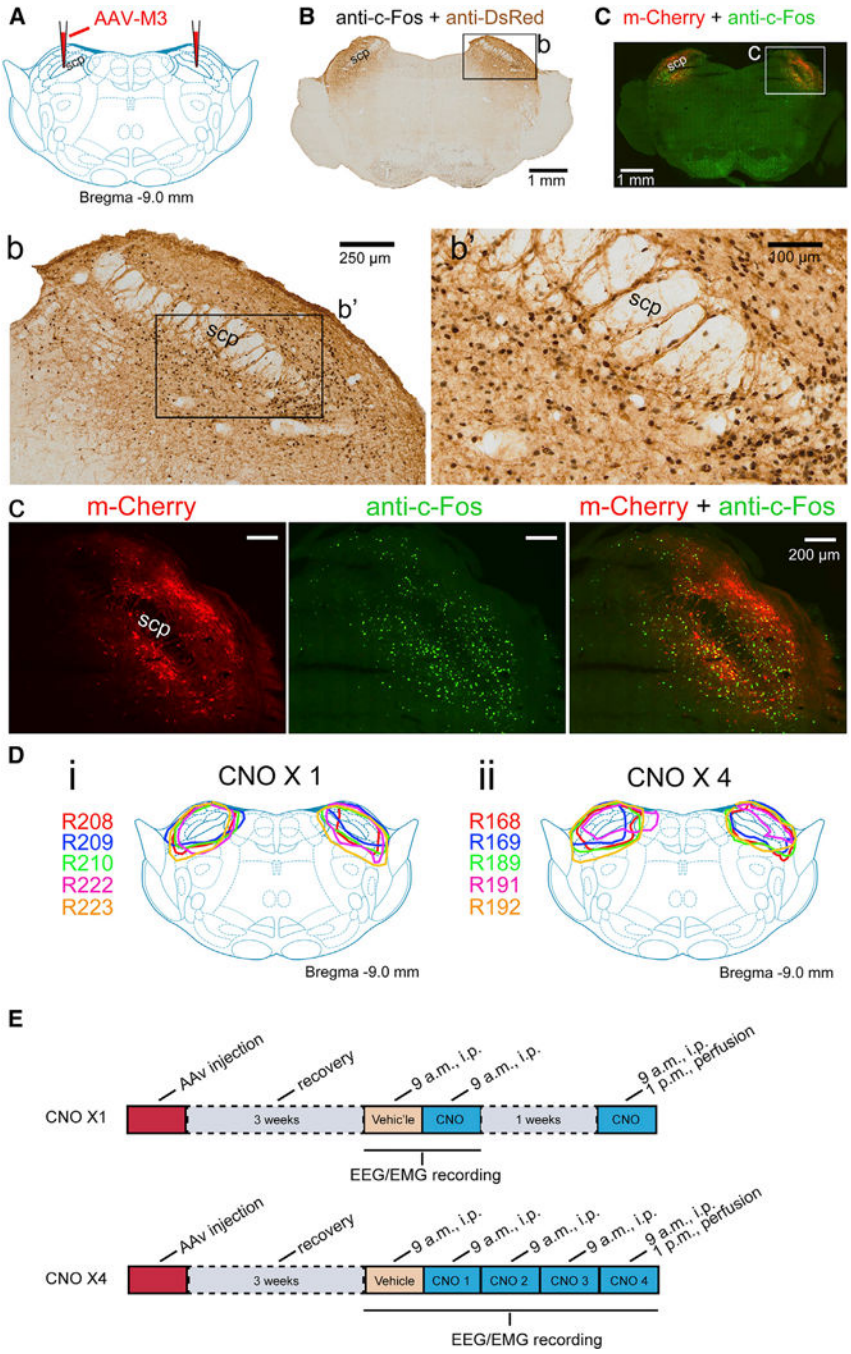

Figure 1. Expression of the AAV-hM3Dq Receptors in PB Neurons

(A) Coronal section showing the injection sites of AAV-hM3Dq-mCherry in the PB. (B and C) Bilateral expression of the hM3Dq receptors in the PB are shown by dsRed-immunostaining (B, brown color) or by native fluorescent mCherry (C, red color) at 594 nm. CNO induced c-Fos expression (black color in B; green color in C) in the PB. The boxed region in (B) is enlarged in (b), and the boxed region in (b) is enlarged in (b'). (c) shows single-channel-acquired fluorescent photos and merged photo of the square region in (C).

(D) Expression of hM3Dq receptors in PB from each cases are outlined in (i) (single CNO i.p. injection at 9 a.m.) and (ii) (4 consecutive days i.p. injection at 9 a.m.). scp, superior cerebellar peduncle.

(E) Timeline of procedures on single CNO treatment (CNO × 1) and four repeated CNO treatment (CNO × 4) animals.

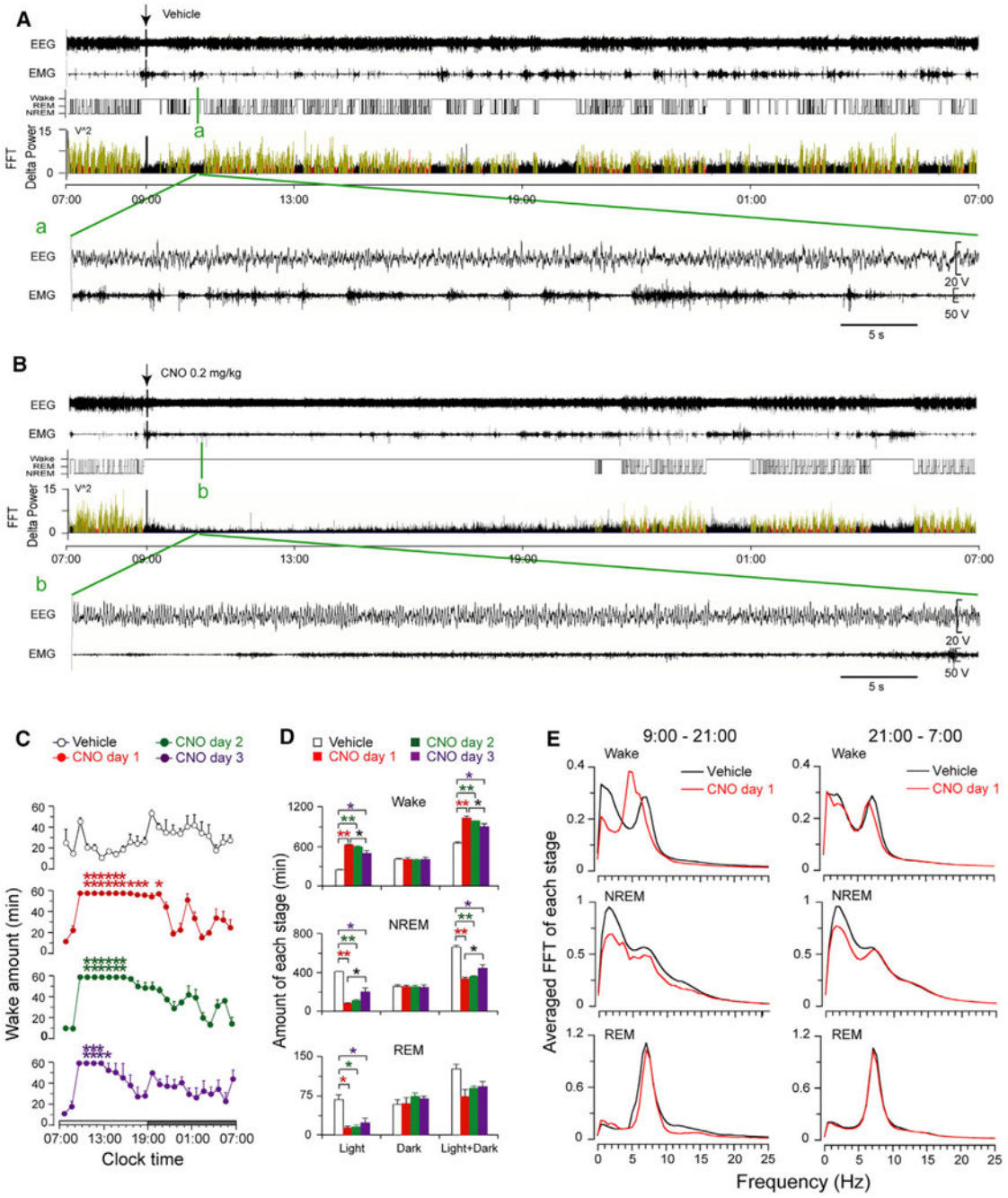

Figure 2. PB Activation Induces a Long Continuous Wakefulness

(A and B) Examples of 24-hr EEG/EMG recordings and corresponding hypnograms and FFT delta power following vehicle (A) or CNO (B; CNO, 0.2 mg/kg, i.p. at 9 a.m.) administration in the same rat with bilateral hM3Dq receptors inserted in the PB. Compared with saline injection, CNO injection induced almost 11 hr uninterrupted wakefulness. (a) and (b) show 1-min segments of EEG, and EMG traces following vehicle or CNO injection (green vertical line on the hypnogram in A and B), respectively, show spontaneous and CNO-induced wakefulness. Black, wakefulness; red, REM sleep; yellow, NREM sleep.

(C) Time course changes of wakefulness produced by saline and three consecutive CNO (0.2 mg/kg) injections at 9 a.m. Open and filled circles represent the hourly mean ± SEM of wakefulness by vehicle and CNO injections (red, green, and purple circles represent day 1, day 2, and day 3 CNO injection data, respectively). *$p < 0.05$; **$p < 0.01$.
(D) Total amounts of wake, NREM, and REM sleep in light, dark, and light + dark period (mean ± SEM) of each treatment (red, green, and purple columns represent day 1, day 2, and day 3 CNO injection data, respectively). *$p < 0.05$; **$p < 0.01$.
(E) Averaged FFT of wake, NREM, and REM sleep during the 12 hr (9 a.m.–9 p.m.) after first CNO injection and during the subsequent 10 hr (9 p.m.–7 a.m.).

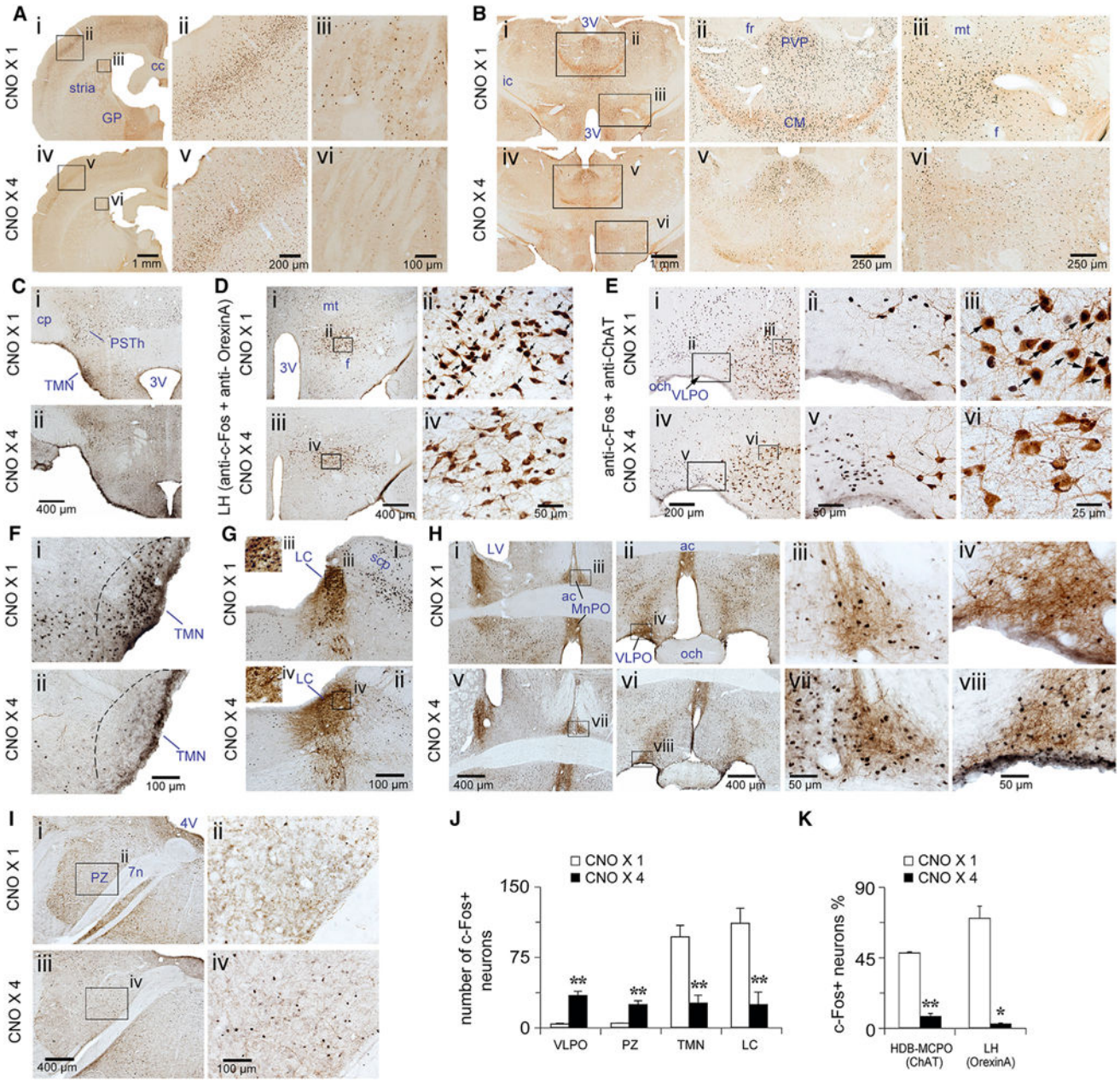

Figure 3. Effects of Single and Repeat Activation of PB on Arousal Sleep-Active Systems

(A) Representative photomicrographs of c-Fos (black color) and dsRed (brown color) immunostaining in the cerebral cortex and striatum of single CNO treatment (CNO × 1; i–iii) and fourth CNO injection (CNO × 4; iv–vi). ii, iii and v, vi are magnified views of the rectangular boxes marked in i and iv, respectively.

(B) Representative photomicrographs of c-Fos (black color) and dsRed (brown color) immunostaining in the thalamus and hypothalamus of single CNO injection (CNO × 1; i–iii) and fourth CNO injection (CNO × 4; iv–vi). ii, iii and v, vi are magnified views of the rectangular areas marked in i and iv, respectively.

(C) Representative photomicrographs of c-Fos (black color) and dsRed (brown color) double immunostaining in the PSTh of single CNO (CNO × 1; i) and fourth CNO injection (CNO × 4; ii).
(D) Representative photomicrographs of c-Fos (black color) and orexin A (brown color) double immunostaining in the LH of single CNO treatment (i and ii) and four times CNO-administered rats (iii and iv). ii and iv are high-magnification views of the rectangular areas marked in i and iii, respectively. Arrows in ii indicate the c-Fos and orexin A double-stained cells.
(E) Representative photomicrographs of c-Fos (black color) and ChAT (brown color) double immunostaining in the VLPO and BF cholinergic neurons of single CNO treatment (i–iii) and four times CNO-administered rats (iv–vi). ii, iii and v, vi are high-magnification views of the rectangular areas marked in i and iv, respectively. Arrows in iii indicate the c-Fos and ChAT double-stained cells.
(F) Representative photomicrographs of c-Fos (black color) and dsRed (brown color) double immunostaining in the TMN of single CNO treatment (i) and fourth CNO-administered rats (ii). The dashed lines outline the TMN area.
(G) Representative photomicrographs of c-Fos (black color) and TH (brown color) double immunostaining in the LC of single CNO treatment (i) and fourth CNO injection (ii). The insert pictures iii and iv are high-magnified images from the rectangular areas marked in i and ii, respectively.
(H) c-Fos (black color) and dsRed (brown color) double immunostaining in the POA (Bregma −0.12) by single CNO treatment (i–iv) and fourth CNO injection (v–viii). iii, iv and vii, viii, are high magnification of the rectangular areas marked in i, ii and v, vi, respectively.
(I) c-Fos (black color) and dsRed (brown color) immunostaining in the PZ of single CNO treatment (i and ii) and four times CNO-administered rats (iii and iv). ii and iv are high-magnification views of the rectangular areas marked in i and iii, respectively.
(J) The number of c-Fos-immunoreactive neurons in VLPO, PZ, TMN, and LC after single CNO or fourth CNO treatments. Values are means ± SEM. *$p < 0.05$; **$p < 0.01$.
(K) The percentage of c-Fos expression in BF ChAT-positive neurons and in LH orexin A-positive neurons. Values are means ± SEM. *$p < 0.05$; **$p < 0.01$. 3V, third ventricle; 4V, fourth ventricle; 7n, facial nerve; ac, anterior commissure; cc, corpus callosum; ChAT, choline acetyltransferase; CM, central medial thalamic nucleus; f, fornix; fr, fasciculus retroflexus; GP, globus pallidus; ic, internal capsule; LC, locus coeruleus; LH, lateral hypothalamus; LV, lateral ventricle; MnPO, median preoptic nucleus; mt, mammillothalamic tract; och, optic chiasm; PSTh, parasubthalamic nucleus; PVP, paraventricular thalamic nucleus, Post; PZ, parafacial zone; scp, superior cerebellar peduncle; stria, striatum; TMN, tuberomammillary nucleus; VLPO, ventrolateral preoptic nucleus.

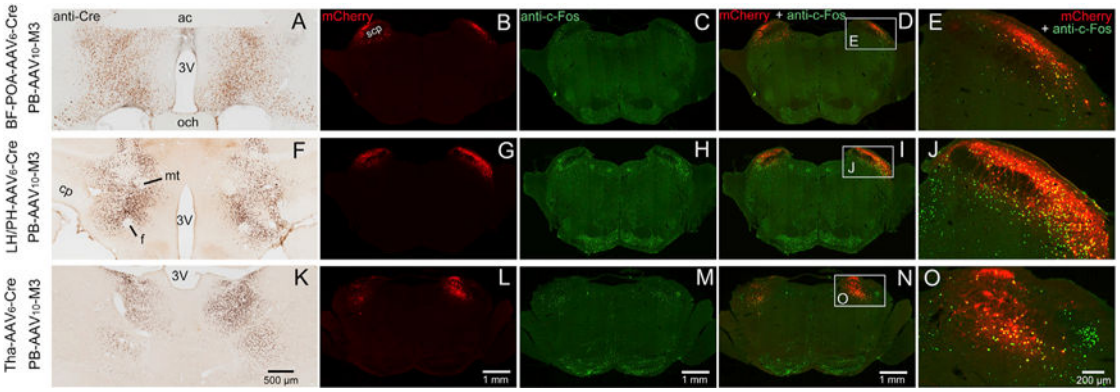

Figure 4. Retrograde-Driven Expression of hM3Dq Receptors in PB Neurons Projecting to the POA and BF, Lateral and Posterior Hypothalamus, and Thalamus

(A, F, and K) Cre immunostaining of AAV_6-cre expression in the POA and basal forebrain (POA+BF) (A), lateral and posterior hypothalamus (LH/PH) (F), and thalamus (Tha) (K). (B–E, G–J, and L–O) cre-dependent expression of AAV-hM3Dq-mCherry (red) and CNO-induced c-Fos in the PB (green).

The top, middle, and bottom panels indicate PB-BF-POA, PB-LH/PH, and PB-Tha pathway. cp, cerebral peduncle.

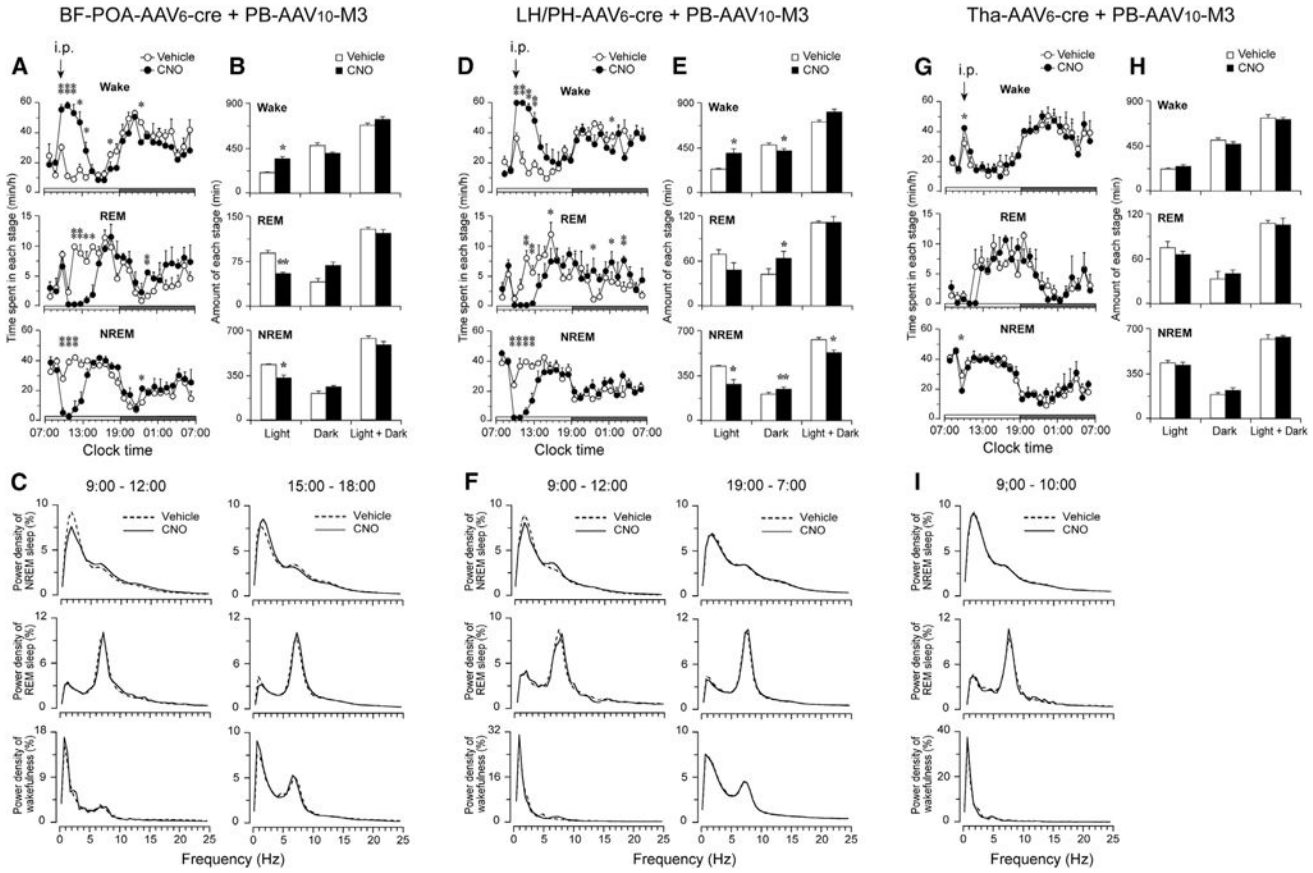

Figure 5. Effects of Activation of PB-BF-POA, PB-LH/PH, and PB-Tha Pathways on Wake Behavior and FFT

(A, D, and G) Time course changes of wake, REM, and NREM sleep produced by saline or CNO (0.2 mg/kg) injection at 9 a.m. in PB-BF-POA, PB-LH/PH, and PB-Tha pathways, respectively. Open and filled circles are saline and CNO groups. Data are represented by hourly mean ± SEM of wake, REM, and NREM sleep.

(B, E, and H) Total amount of wake, NREM, and REM sleep (mean ± SEM) during the light and dark period and 24 hr of each group.

(C) Relative averaged EEG power density of each stage during the first 4 hr after saline or CNO injection or in the succeeding period of time from 3 p.m. to 6 p.m. of PB-BF-POA pathway group.

(F) Relative averaged EEG power density of NREM sleep during first 4 hr after saline or CNO injection and during subsequent night of PB-LH/PH pathway group.

(I) Relative averaged EEG power density of NREM sleep during first 2 hr after saline or CNO injection in PB-Tha pathway group.

*$p < 0.05$; **$p < 0.01$.

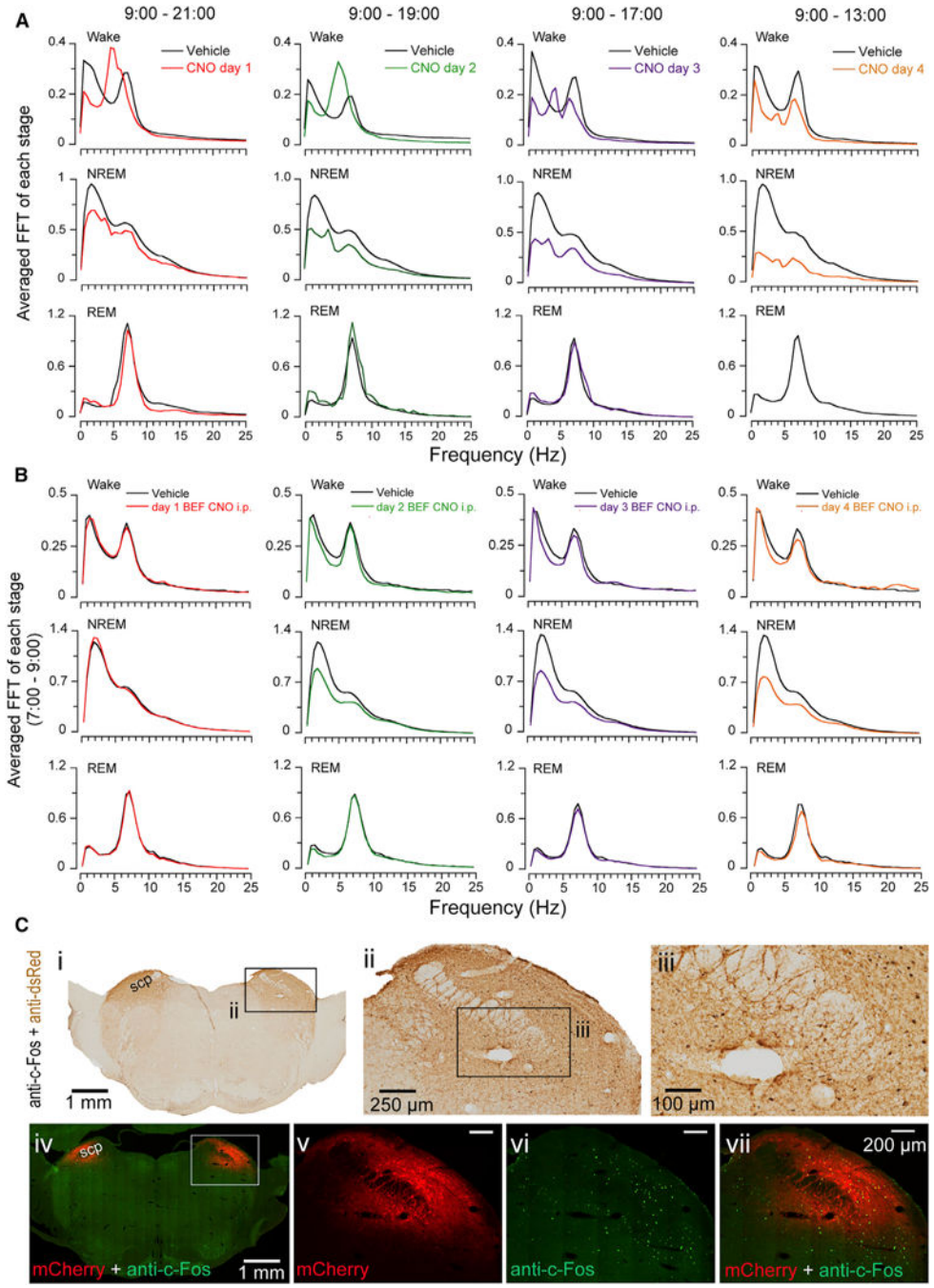

Figure 6. Effects of Repeated PB Activation on Sleep-Wake FFT

(A) Wake, NREM sleep, and REM sleep FFT induced by PB activation at 9 a.m. in days 1–4.

(B) Wake, NREM, and REM sleep FFT during 2 hr prior to CNO injection in days 1–4.

(C) Expression of M3 receptors and c-Fos expression in the PB after fourth CNO injection. (ii) shows higher magnification of the square region indicated in (i). (iii) shows higher magnification of the square region indicated in (ii). (v), (vi), and (vii) show single-channel-acquired fluorescent photos and their merged photo of the square region indicated in (iv).

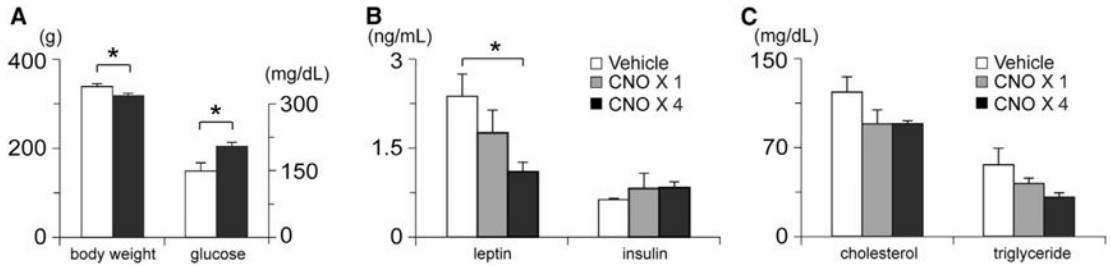

Figure 7. Effect of Extended Wakefulness on Body Weight and Metabolic Parameters

(A) Changes in body weight and blood glucose (mean ± SEM) following four consecutive CNO injections in rats with bilateral hM3Dq receptors in PB. (B and C) Changes in leptin, insulin, cholesterol, and triglyceride (mean ± SEM) following single and four CNO injections in rats with bilateral hM3Dq receptors in PB.

*$p < 0.05$.